MODEL BASED FAULT DIAGNOSIS OF THE MAIN DRIVE OF A HORIZONTAL MILLING MACHINE

P. Wanke

Institut of Automatic Control, Laboratory of Control Systems and Process Automation, Technical University Darmstadt, Landgraf-Georg-Str. 4, D-6100 Darmstadt, Germany

Abstract

The early detection and localization of faults in machines and drives is of primary interest to make further improvement of the reliability and saftey. This paper presents a new approach in fault diagnosis and supervision of main drives with elastic components.

The supervision of drives with additional sensors for temperature, pressures or vibrations is usually expensive. Currently, internal process faults are only detected partially and at a rather late stage, by generating alarms if certain limits of the measured signals are exceeded or limit switches stop the machine tool. A process model based approach for fault diagnosis was developed. A dynamic model of the main drive was derived and together with easily measurable signals of the drive, like current and speed, physical parameters can be estimated. Changes of those process parameters are the symptoms for a diagnostic inference mechanism.

Experimental results with least squares parameter estimation in the form of disrete square root filters are shown.

Keywords

Fault detection, machine tool, main drive, modelling, parameter estimation, process monitoring.

1. Introduction

The aim of supervision of machine tools is to detect changes and faults during normal operation and to take proper actions at an early stage to avoid a damage of the process. Until now, machine tool supervision is mainly performed by limit value checking of some measurable variables. However, internal process faults may then only be detected too late.

To get further insight of the internal process behaviour without the use of additional sensors, one needs a dynamic mathematical process model, see e.g. Isermann, et. al. /1/, for each drive of the machine tool. Generally, the model can be described by

$$\underline{Y} = f(\underline{U}, \underline{N}, \underline{\Theta}) \qquad (1)$$

$\underline{U}(t)$ and $\underline{Y}(t)$ are measurable input and output signals, $\underline{N}(t)$ disturbance signals (noise) and $\underline{\Theta}(t)$ constant or slowly time varying process parameters.

If a fault appears in the process, depending on its type, this will cause changes $\Delta\underline{\Theta}(t)$ of the process parameters. These changes will lead to changes $\Delta\underline{Y}(t)$ of the mesurable variables due to certain dynamics. The actual process parameters $\underline{\Theta}(t)$ can be estimated via recursive identification of continuous-time process models.

By these model oriented detection procedures, several process faults may be detected and localized by using only few robust sensors and the physically based dynamic causalities between the signals, see Willsky /2/, Isermann /3/.

In case of an early failure hint, one may then take individual actions of maintenance, while before were taken on regular maintenance intervals.

2. Theoretical modelling of the main drive

Fig. 1 shows the main drive of a horizontal milling machine MAHO MC5. This main drive consists of a motor, a belt drive, a gear, some shafts and a work spindle. The motor speed is in the range from 300 rpm up to 5000 rpm. Using four transfer factors (0.065, 0.206, 0.506 and 1.602), a spindle speed in the range from 20 rpm up to 6000 rpm is obtained. These transfer factor may directly computed by multiplying gear and belt drive transmission factor.

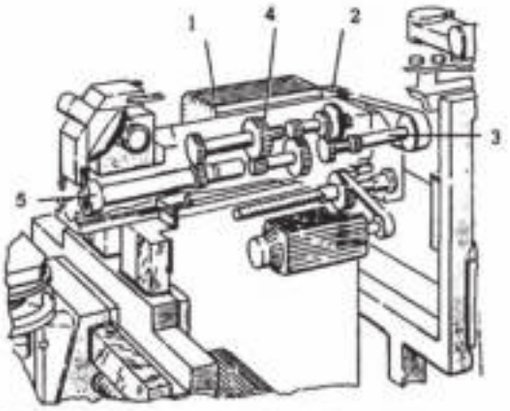

Fig. 1 Main drive of a flexible milling center
1 d.c. motor, 2 belt drive, 3 shaft,
4 gear and 5 work spindle

An equivalent scheme of the dynamic behaviour of the main drive is shown in Fig. 2. The main drive may be divided in an electrical subsystem (motor), a mechanical subsystem (drive chain) and working process (e. g. milling). However, this paper dials only with the modelling and identification of the electrical and mechanical subsystems. For failure respectively tool wear detection of the cutting process see Reiß, et. al. /4/, or Fuchs, et. al. /5/.

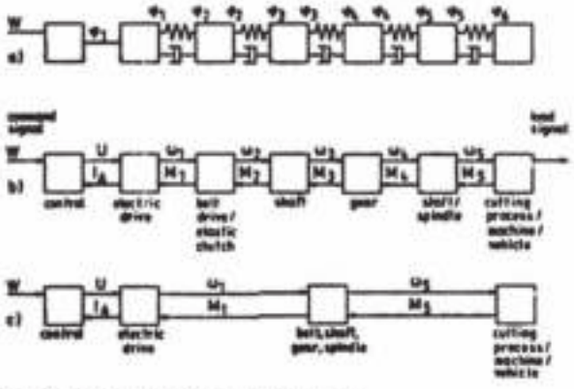

Fig. 2 Schemes of the main drive, /1/
a) Rotating two-mass-damper systems
b) Representation in form of four terminal networks
c) Simplified model for parameter estimation

2.1. Electrical subsystem

The dynamic behavior of the d.c. motor can be described by the two equations

$$L \frac{d I_A(t)}{d t} = - R\, I_A(t) - \Psi\, \omega_1(t) + U_A(t) \qquad (2)$$

$$J_1 \frac{d \omega_1(t)}{d t} = \Psi\, I_A(t) - M_L(t) \qquad (3)$$

with L armature inductive resistance,
R armature resistance,
J_1 moment of inertia,
Ψ flux linkage,
$I_A(t)$ armature current,
$U_A(t)$ armature voltage,
$\omega_1(t)$ motor speed and
M_L load torque.

During operation with field shunting the flux linkage Ψ depends on the exciting current $I_E(t)$

$$\Psi = f(I_E). \qquad (4)$$

This influence can be taken out of the specification sheet of the manufacturer.

2.2 Mechanical subsystem

According to Fig. 1 the drive chain consist of belt drive, shaft, gear box and work spindle. Assuming small deviations $\varphi(t)$ from steady-state, for each of this mechanical elements the dynamic behaviour may be modeled by an elastic two-mass-damper system, equivalent to Fig. 3.

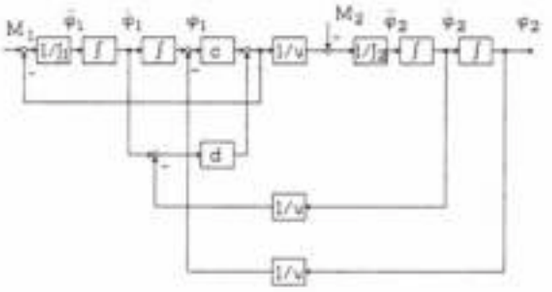

Fig. 3 Block diagram of a two-mass-damper system,
with J_1 J_2 moments of inertia,
c d spring and damping factor,
M_1 M_2 torques and
v transfer factor.

As also shown in Wanke and Reiß /6/, the state space model of the two-mass-damper system is given by

$$\begin{bmatrix} \dot{\omega}_1 \\ \dot{\varphi}_1 \\ \dot{\omega}_2 \\ \dot{\varphi}_2 \end{bmatrix} = \begin{bmatrix} -d/J_1 & -c/J_1 & d/vJ_1 & c/vJ_1 \\ 1 & 0 & 0 & 0 \\ d/vJ_2 & c/vJ_2 & -d/v^2J_2 & -c/v^2J_2 \\ 0 & 0 & 1 & 0 \end{bmatrix} \begin{bmatrix} \omega_1 \\ \varphi_1 \\ \omega_2 \\ \varphi_2 \end{bmatrix} + \begin{bmatrix} 1/J_1 & 0 \\ 0 & 0 \\ 0 & -1 \\ 0 & 0 \end{bmatrix} \begin{bmatrix} M_1 \\ M_2 \end{bmatrix} \qquad (5)$$

with $\varphi_{1/2}$ input/output rotation angle and
$\omega_{1/2}$ input/output speed.

Models for the mechanical elements of the main drive are summarized in Table 1, see also /1/. Setting the transfer factor v in Eq. (5) to

$$v_S = 1, \qquad (6)$$

one directly obtains the state-space representation of the shaft.

In case of the belt drive the transfer factor v is set to

$$v_B = r_2/r_1, \qquad (7)$$

where r_1 and r_2 are the radius of each belt pulley respectively. Additionally a slip s must be taken in account for the state space representation of the belt.

The transfer factor v_G depends on the position of the gear shifting switch.

Process	Differential Equation
shaft 	$J_2\ddot{\varphi}_2(t) + c_S[\varphi_1(t) - \varphi_2(t)] + d_S[\dot{\varphi}_1(t) - \dot{\varphi}_2(t)] - M_2(t)$ $J_1\ddot{\varphi}_1(t) + c_S[\varphi_2(t) - \varphi_1(t)] + d_S[\dot{\varphi}_2(t) - \dot{\varphi}_1(t)] + M_1(t)$
belt 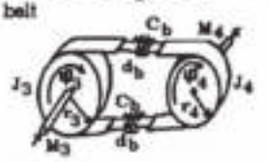	$J_3\ddot{\varphi}_3(t) + c_B[v_0\varphi_4(t) - \varphi_3(t)] + d_B[v_0\dot{\varphi}_4(t) - \dot{\varphi}_3(t)] + M_3(t)$ $J_4\ddot{\varphi}_4(t) + c_B v_0[\varphi_3(t) - v_1\varphi_4(t)] + d_B v_0[\dot{\varphi}_3(t) - v_1\dot{\varphi}_4(t)] - M_4(t)$
gear 	$J_5\ddot{\varphi}_5(t) + c_g[\varphi_6(t)/v_g - \varphi_5(t)] + d_g[\dot{\varphi}_6(t)/v_g - \dot{\varphi}_5(t)] + M_5(t)$ $J_6\ddot{\varphi}_6(t) + c_g/v_g^2[v_g\varphi_5(t) - \varphi_6(t)] + d_g v_g^2[v_g\dot{\varphi}_5(t) - \dot{\varphi}_6(t)] - M_6(t)$

Table 1: Mathematical models of the mechanical drive elements (c_j spring rate, d_j damper rate, v_j transfer factor, J_j moment of inertia)

Connecting the single elements by four terminal networks, Fig. 1, the overall model of the drive chain is obtained. Thus, a state vector of 10^{th} order

$$\underline{x}^T = (\varphi_1\ \dot{\varphi}_1\ \varphi_2\ \dot{\varphi}_2\ \varphi_3\ \dot{\varphi}_3\ \varphi_4\ \dot{\varphi}_4\ \varphi_5\ \dot{\varphi}_5) \tag{8}$$

may be defined.

2.3 Overall model of the main drive

Connecting the electrical subsystem, Eq. (2) and (3), and the mechanical subsystem, Eq. (8), the overall model of the main drive is obtained. A state vector of 11^{th} order

$$\underline{x}^T = (I_A\ \varphi_1\ \dot{\varphi}_1\ \varphi_2\ \dot{\varphi}_2\ \varphi_3\ \dot{\varphi}_3\ \varphi_4\ \dot{\varphi}_4\ \varphi_5\ \dot{\varphi}_5) \tag{9}$$

may be derived and the overall state model becomes

$$\dot{\underline{x}}(t) = \underline{A}\,\underline{x}(t) + \underline{b}u(t) + \underline{f}z(t) \tag{10}$$

with $u(t) = \Delta U_A(t)$, $z(t) = \Delta M_L(t)$.

$\Delta U_A(t)$ and $\Delta M_L(t)$ represent variations of the d.c. motor voltage and the load torque. The load torque depends on the working process, like milling or drilling. In the remaining part of this paper, the influence of the working process will not be considered. Only failures during no-load operations are investigated.

3. Parameter estimation of continous-time processes

Basically, failure detection is the combination of theoretical modelling and parameter estimation of continuous-time models.

According to section 2, the structure of the models is known and the parameters Θ_j have to be estimated in order to detect changes of the main drive during testruns.

3.1 Basic equations

With reference to Eq. 1 one can abbriviate:

$$y(k) = \underline{\psi}^T(k)\,\underline{\Theta} \tag{11}$$

where $\underline{\psi}$ is the observation vector, k is the sample of measurement and $\underline{\Theta}$ is the parameter vector, with

$$\underline{\psi}^T(k) = (-y(k), \ldots, -y^{(n)}(k), u(k), \dot{u}(k), \ldots, u^{(m)}(k)) \tag{12}$$

and $$\underline{\Theta}^T = (a_1, \ldots, a_n, b_0, \ldots, b_m) \tag{13}$$

The unknown process parameters $\underline{\Theta}$ are obtained by minimizing the loss function

$$V = \sum_{k=0}^{N} e^2(k) = \underline{e}^T\underline{e}, \text{ with} \tag{14}$$

$$e(k) = y(k) - \underline{\psi}^T(k)\,\hat{\underline{\Theta}} \tag{15}$$

where $\hat{\underline{\Theta}}$ represents the estimated values of $\underline{\Theta}$. Factorizing the so called information matrix $\underline{Q}$

$$\underline{Q}(N) = \underline{\Psi}^T(N)\,\underline{\Psi}(N) \tag{16}$$

in two upper triangular square roots by using the Householder transformation a numerical optimized estimation method called discrete square root filter (DSFI), see Isermann /7/, is given.

3.2 Determination of the signals derivatives

As only the input and output signals u and y, can be measured, their derivatives $\dot{y}, \ddot{y}, \ldots$ and $\dot{u}, \ddot{u}, \ldots$ must be determined in a different way. For this task, the method of state-variable-filtering (SVF) is well suited, see Young /8/. The SVF is implemented by a programmable digital filter F(s), Fig. 4

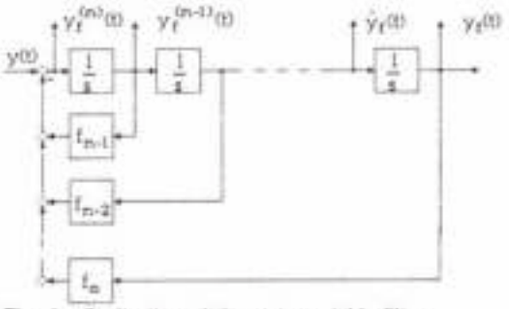

Fig. 4: Realization of the state-variable-filter

For each filter the transfer function is given by:

$$F(s) = \frac{y_F(s)}{y(s)} = \frac{1}{f_0 + f_1 s + \ldots + f_q s^q} \tag{17}$$

The parameters $f_0, f_1, \ldots f_q$ are designed via Butterworth-filter-characteristics, see Peter and Isermann /9/. The filtered signals $y_f(1), \ldots, y_f(q)$ may then be fed into the observation matrix $\underline{\Psi}(k)$.

4. Physically based model reduction

As shown earlier, the main drive of the machine tool may be represented by a 11^{th} order model which is too complex to be analysed by only measuring input and output data. With regard to subsequent fault diagnosis on the main drive, one has to develop a reduced model descri-

bing the essential dynamic behaviour.

Considering the mechanical subsystem, one can reduce the model of 10th order by neglecting these elements with a large stiffness. Therefore, spring and damper factor and also the moments of inertia are calculated for each element by specification sheets of the manufacturer. Since the elasticity of shaft and work spindel is small compared to the one of belt drive and gear box, one neglect these two elements. Thus, one gets a 6th order model. Simulation results may show good agreements between the signals of both the original and the reduced model.

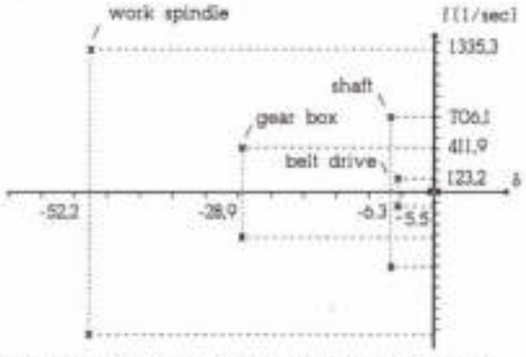

Fig. 5: Pole configuration of the mechanical subsystem

Fig. 5 shows the pole configuration of the 10th order model. The transfer factor v_g is set to $v_g = 0.065$. The two roots in the zero point represent the behaviour of an inert mass in continued acceleration of an input torque. The conjugate-complex roots represent the characteristic oscillations of each mechanical element. This pole configuration proves that indeed, gear box and belt drive are the elements with the largest elasticity, which need to be considerd in the 6th order model.

In a second step, the elasticities of both elements may be lumped together leading to an again reduced model. This now 4th order model corresponds to the two-mass-damper system shown in Fig. 3. Considering the belt drive as the element with the largest elasticity, see Fig. 5, one obtains the parameters for the reduced model according to Eq. (5), see Table 2.

$J_1 = J_M + J_{B1}$	(moment of inertia at the pinion end)
$J_2 = J_S + J_{G2} + (J_{B2} + J_W + J_{G2})/v_G$	(Moment of inertia at the drive side)
$c = c_B$	(spring factor)
$d = d_B$	(damper factor)
$v = v_B v_G$	(transfer factor)
ω_1	(motor speed)
ω_5	(work spindle speed)

Table 2: Parameters of the reduced model

The eigenfrequency of the resulting model is given by

$$f = \frac{1}{2\pi} \sqrt{c / v J_2} \tag{18}$$

Comparing the pole configuration of the models of 10th and 4th order, see Fig. 5 and 6, one finds that the four roots of the reduced model are in a good accordance with the four dominant roots of the overall model.

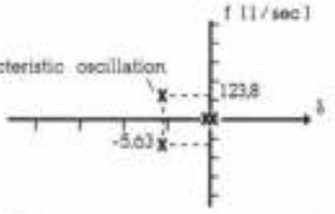

Fig. 6: Pol configuration of the reduced model of 4th order

5. Identification of the parameters of the reduced model

5.1. Equations for the parameter estimation

To estimate the parameters of the d.c. motor Eq. (2) is used. One gets

$$U_A(t) = \Theta_1 \omega_1(t) + \Theta_2 I_A(t) + \Theta_3 \dot{I}_A(t) \tag{19}$$

with $\Theta_1 = \Psi$, $\Theta_2 = R$, $\Theta_3 = L$.

Putting the parameters of Table 2 in Eq. (5). One gets

$$\dot{\omega}_1(t) = -\frac{d}{J_1}\omega_1(t) - \frac{c}{J_1}\varphi_1(t) + \frac{d}{vJ_1}\omega_5(t) + \frac{c}{vJ_1}\varphi_5(t) + \frac{1}{J_1}M_1(t) \tag{20}$$

and

$$\dot{\omega}_5(t) = \frac{d}{vJ_2}\omega_1(t) + \frac{c}{vJ_2}\varphi_1(t) - \frac{d}{v^2J_2}\omega_5(t) - \frac{c}{v^2J_2}\varphi_5(t) - M_2(t) \tag{21}$$

The torque M_1 in Eq. (20) depends on the motor torque minus a friction M_F, hence

$$M_1(t) = \Psi I_A(t) - M_F \tag{22}$$

The torque M_2 in Eq. (21) correspond to the reacting torque M_L of the working process and is set to

$$M_2(t) = 0, \tag{23}$$

because of no-load operations during parameter estimation. Adding Eq. (20) and Eq. (21) and regarding Eq. (22) and Eq. (23), one gets

$$\Psi I_A(t) - M_F = \Theta_4 \dot{\omega}_1(t) + \Theta_5 \dot{\omega}_5(t) \tag{24}$$

with $\Theta_4 = J_1$ and $\Theta_5 = vJ_2$.

The parameter Ψ on the left side of Eq. (24) must be estimated previously, see Eq. (19), or taken out of the specification sheet of the manufacturer.

Putting Eq. (23) in Eq. (21) the balance of torque on the work spindle yields

$$\varphi_5(t) = \Theta_6 \omega_1(t) + \Theta_7 \varphi_1(t) - \Theta_8 \omega_5(t) - \Theta_9 \dot{\omega}_5(t) \tag{25}$$

with $\Theta_6 = \frac{d}{c}v$, $\Theta_7 = v$, $\Theta_8 = \frac{d}{c}$, $\Theta_9 = \frac{J_2}{c}v^2$

By using the inverse relationship

$$\underline{p} = f^{-1}(\underline{\theta}) \tag{26}$$

the coefficients $\underline{p}$ can be determined uniquely and the identifiability of the reduced main drive model can be shown. The coefficientes yield to

$$\begin{aligned} v &= \theta_7 \\ J_1 &= \theta_4 \\ J_2 &= \theta_5 / \theta_7 \\ c &= \theta_5 \theta_7 / \theta_9 \\ d &= \theta_5 \theta_7 \theta_8 / \theta_9. \end{aligned} \tag{27}$$

5.2. Experimental results

First experiments have shown that, if the transfer factor v_G is constant, the friction M_F hardly depends on speed variations. Hence, for the actual transfer factor v_G, a constant friction M_F is determined in a preliminary examination during a period of constant speed.

The excitation of the estimation cycle is about 15 step inputs of motor speed. The corresponding measured signal of the work spindle speed ω_5 (t) and his first derivative are shown in Fig. 7 for four step inputs.

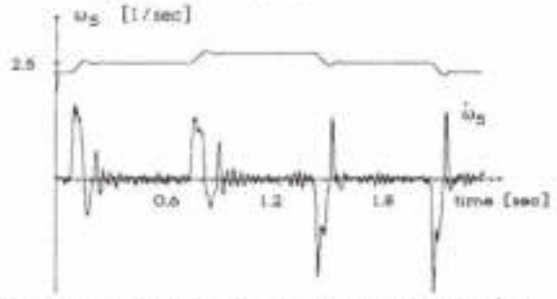

Fig. 7 Work spindle speed $\omega_5(t)$ and first derivative $\dot{\omega}_5(t)$

The process signals $\omega_1(t)$ and $\omega_5(t)$ were measured with a sampling rate of $T_0 = 0.001$ sec and then filtered by a state-variable filter of 6th order described in section 3.

Some estimated physical coefficients are shown in Fig. 8 up to Fig. 12. For these examinations Eq. (25) is derivated as the angular position φ_1 (t) can not be measured at this time due to a sensor inability.

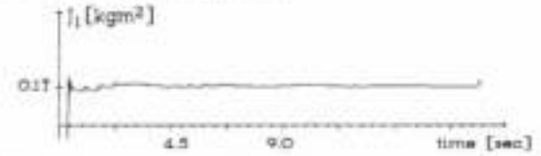

Fig. 8 Moment of inertia J_1

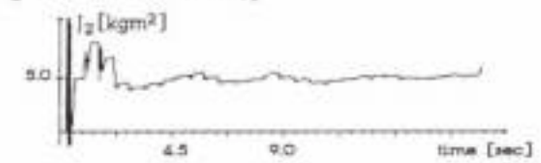

Fig. 9 Moment of inertia J_2

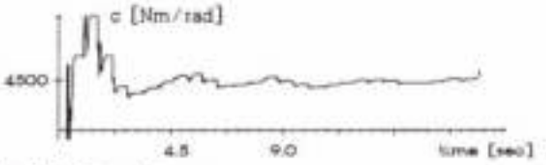

Fig. 10 Spring factor c

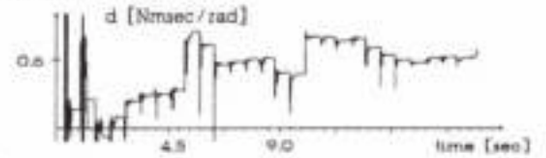

Fig. 11 Damping factor d

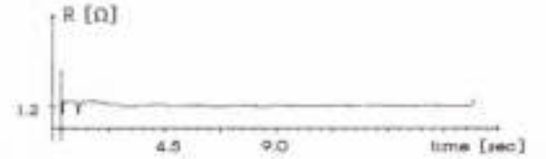

Fig. 12 Armature resistance R

The parameters are in a good accordance to the correct physical values of the machine.

5.3. Fault diagnosis

First results of the fault diagnosis of the main drive are shown in Fig. 13 up to Fig. 15. This results are based on a simulation of the model Eq. (10). The state variables are used as input and output signals for the parameter estimation. The simulations were carried out under different conditions:

1. Reference simulation (with calculated parameters),
2. Simulation with increased armature resistance,
3. Simulations with increased modulus of elasticity of the belt drive and
4. Simulations without initial tension of the belt drive.

The estimated process parameters or process coefficients represent features of the process. Their changes in comparison to the normal behaviour may be used as fault symptoms. The knowledge-based fault diagnosis, which is not especially treated in this paper, is designed to interprete this symptoms, see Isermann, et. al. /1/, Freyermuth and Neumann /10/. Similar experimental researches are done in the field of robots, see Freyermuth /11/.

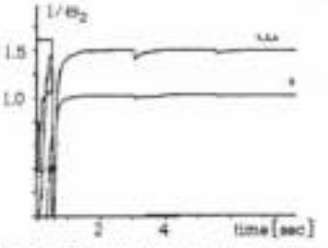

Fig. 13 Estimated parameter $1/\theta_2$

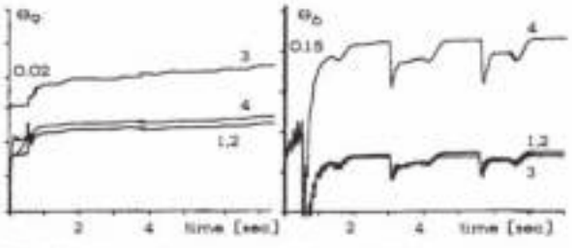

Fig. 14 Estimated parameter a) Θ_c and b) Θ_δ

Fig. 13 shows the inverted parameter Θ_2, which represents the armature resistance. This parameter only changes in case of simulation-condition 2. The other simulated failures does not depend on Eq. (2) of the d.c. motor. Fig. 14a shows the estimated parameter Θ_9. There are changes in case of the simulation conditions 3 and 4. This effect can be explained looking at the reduced model. The characteristic oscillation depends on the elasticity of the belt drive. The parameter Θ_δ, see Fig. 14b, demonstrate the same effects. Changes depends directly on changes of the spring factor c. Table 3 shows examples of the symptoms of different failure states, depending on changes of the estimated parameters.

Simulation condition:		Θ_2	Θ_δ	Θ_9
	2	++	o	o
	3	o	-	++
	4	++	o	+

Table 3: Symptoms for fault diagnosis (- decrease, + increase, o constant)

Acknowledgement:

This paper presents results of a compound research project, which is sponsored by the "German Bundesministerium für Forschung und Technologie (BMFT)", in the field of the project "Fertigungstechnik (PFT)" with the project number 02FT46068, managed by the "Kernforschungszentrum Karlsruhe".

Conclusions:

The modelling of the main drive of a milling machine was described. A reduced model, appliable for identification of the physical coefficients was given. A least squares parameter estimation method was shown to calculate some coefficients. Experimental results on a machining center MAHO MC5 show some estimated process coefficients. Simulations show the fitness of the method for fault diagnosis.

References:

/1/ Isermann, R., Appel, W., Freyermuth, B., Fuchs, A., Janik, W., Neumann, D., Reiß, T., Wanke, P. "Model based fault diagnosis and supervision of machines and drives". 11th IFAC World Congress, 13.-17. August 1990, Tallinn, USSR.

/2/ Willsky, A.S. "A survey of design methods for failure detection systems". Automatica, 12.

/3/ Isermann, R. "Process fault detection based on modeling and estimation methods - a survey". Automatica, Vol. 20.

/4/ Reiss, Th., Wanke, P., Isermann, R. "Model based fault diagnosis of a flexible milling center". 11th IFAC World Congress, 13.-17. August 1990, Tallinn, USSR.

/5/ Fuchs, A., Janik, W., Isermann, R. "Model based supervision and fault diagnosis of the cylindrical grinding process". XI IMEKO World Congress, Houston, USA.

/6/ Wanke, P., Reiß, T. "Modellgestützte Maschinendiagnose an Haupt- und Vorschubantrieben von Bearbeitungszentren". KfK-AWF Symposium, 10.10.90, Düsseldorf.

/7/ Kaminski, P.G. "Discrete square root filtering: a survey of current techniques", IEEE-Trans. AC-16, pp.727-736.

/8/ Isermann, R. "Identifikation dynamischer Systeme, I und II". Springer-Verlag, 1988.

/9/ Young, P.C. "Parameter estimation for continous-time models - a survey". Automatica, 17, pp. 23-29.

/10/ Peter, K., Isermann, R. "Parameter adaptive control based on continuous-time process models". 11th IFAC World Congress, Tallinn, USSR, 1990.

/11/ Freyermuth, B., Neumann, D. "Ein Konzept zur Gestaltung wissensbasierter Systeme für die Fehlerfrühdiagnose technischer Prozesse". GMAutotech '90, 18.9./19.9.90, Baden-Baden.

/12/ Freyermuth, B. "Online Fehlerfrüherkennung bei Industrieroboter mittels Parameterschätzung und Fehlerklassifikation." VDI-Tagung Schwingungsüberwachung-Maschinendiagnose, Mannheim, 11.10./12.10.90.